1.2-mm Continuum Observations of IRAS Galaxies: Implications for Gas Mass and Cold Dust Component

P. ANDREANI[1], A. FRANCESCHINI[2] and J. ROLAND[3]

[1] ESO; [2] Osservatorio Astronomico di Padova, Italy; [3] Institut d'Astrophysique de Paris, France

Introduction

New fields of research have been opened at ESO with the SEST 15-m antenna (see *The Messenger* No. 57), and in particular we find promising the coupling between this telescope and the MPIfR bolometer because of the very high sensitivity of this instrument. This system will allow the investigation of the continuum emission at millimetric wavelengths of galactic and extragalactic objects.

We have started an observational programme, to be carried out partly with the SEST telescope, to investigate the 1.2-mm continuum emission of a complete sample of galaxies selected from the IRAS Point Source Catalogue (Smith et al., 1987).

Among the important issues which can be addressed from this project, we find of particular interest:

(a) the study of the electromagnetic spectra of galaxies at long wavelengths: late-type galaxies represent the majority of the extragalactic sources detected by the IRAS satellite. Most of their observed emission is thermal and comes from dust in HI clouds heated by the general interstellar radiation field, cold dust in molecular clouds and dust heated by hot stars embedded in compact HII regions.

However, to understand both galactic evolution and star-formation processes, which are strictly connected with the available dust and gas present in the interstellar medium, one needs to know the total amount of these components in the galaxy disks. The true dust column density cannot be properly estimated only by means of the FIR measurements, like those of the IRAS satellite, since they are not sensitive to dust colder than 20 K and the bulk of dust mass is expected to emit at submillimetre and millimetre wavelengths. Continuum flux densities in this spectral range are good tracers of the total dust, gas and molecular mass and can represent an alternative way to estimate these parameters.

(b) galaxy counts at these wavelengths: the source distribution, N(S), and its first and second moments: $I = \int S \cdot N(S) dS$ and $(\Delta I)^2 = \int S^2 \cdot N(S) dS$, provide relevant constraints on models of cosmological evolution of the studied objects. In particular, the fluctuation level generated by unresolved randomly distributed sources, given by the second moment of the N(S) distribution, can significantly constrain the small- and intermediate-scale anisotropies of the Cosmic Microwave Background (CMB) (Franceschini et al., 1989) even at ~1 mm, i.e. near the peak of the CMB.

At present, very few observations are available of the millimetre continuum emission of galaxies and they are mainly biased towards active galaxies (both AGNs and starburst galaxies), because of their enhanced nuclear emission. The only mm measurements available on spiral galaxies are those reported by Chini et al. (1986), but the claimed conspicuous presence of a cold dust component peaking around 200 μm has not been confirmed by other submillimetre observations (Stark et al., 1988; Eales et al., 1989).

The first observations have been performed at the IRAM 30-m telescope. To allow comparison between the mm fluxes with the IRAS observations and to avoid large systematic errors introduced by aperture corrections, the angular dimensions of the galaxies should not exceed the beam width. Therefore, we have chosen galaxies of the sample with optical size comparable with the IRAM 30-m beam width (HPBW = 11″).

The 1.2-mm continuum emission of 7 objects of the sample and 5 other galaxies has been studied and issues on the presence of a cold component of the interstellar medium and dust and gas masses of the disks are preliminarily addressed.

Observations

The observational mode is briefly outlined since most of the performances of the IRAM 30-m antenna are equal to those of the SEST.

The observations have been carried out with the ^{3}He bolometer of the MPIfR fed by the IRAM 30-m telescope at Pico Veleta (Spain) on March 17–18 and May 17–19, 1990.

The position of the sources was found by pointing a nearby radio quasar with strong millimetric fluxes. Pointing accuracy was most of the time better than 2″ and was checked every half hour. Beam-switching is achieved by wobbling the secondary in azimuth ON-OFF the source and nodding the telescope, resulting in a three-beam technique which, therefore, allows comparison between the source signal and that from two nearby empty sky regions. The wobbling amplitude was set to be much larger than the optical radius of the galaxy.

Each source has been observed n · 200 s times with n depending on the expected 1.2-mm intensity. To approximately evaluate the millimetric flux the IRAS 100 μm flux has been extrapolated by assuming a thermal spectrum with spectral index between 1 and 2.

Atmospheric transmission has been monitored by frequent skydips. Uranus, Mars, Neptune and Jupiter have been used as primary calibrators by assuming weighted effective temperatures at this wavelength of 93 ± 1, 200 ± 6, 96 ± 2 and 169 ± 3, respectively (Orton et al., 1986; Gear et al., 1985). The quasars 3C286, 0839 + 187, 0953 + 255, 1156 + 295, 2201 + 315 have been used as secondary calibrators mainly to detect sky variations during the observations.

The overall accuracy on the detected fluxes depends strongly on the atmospheric conditions, being between 10 and 30 %.

Results

Of 12 observed sources (7 belonging to the sample and 5 are isolated objects) 9 have been detected and for the other 3 upper limits were obtained. Figure 1 shows 4 IR/mm spectra, the IR fluxes have been taken from the IRAS Point Source Catalogue (Lonsdale et al., 1989) and have been slightly modified according to the colour and K-corrections (Smith et al., 1987; Lonsdale et al., 1989).

The millimetre values have been also corrected for the overall system response and K-corrections. The former has been evaluated by computing the integral:

$$\Re(w, \alpha) = \int_{\nu_1}^{\nu_2} I_{atm}(\nu, w)\, \mathrm{Y}(\nu) \epsilon(\nu, El) \cdot \left(\frac{\nu}{\nu_0}\right)^{\alpha} d\nu$$

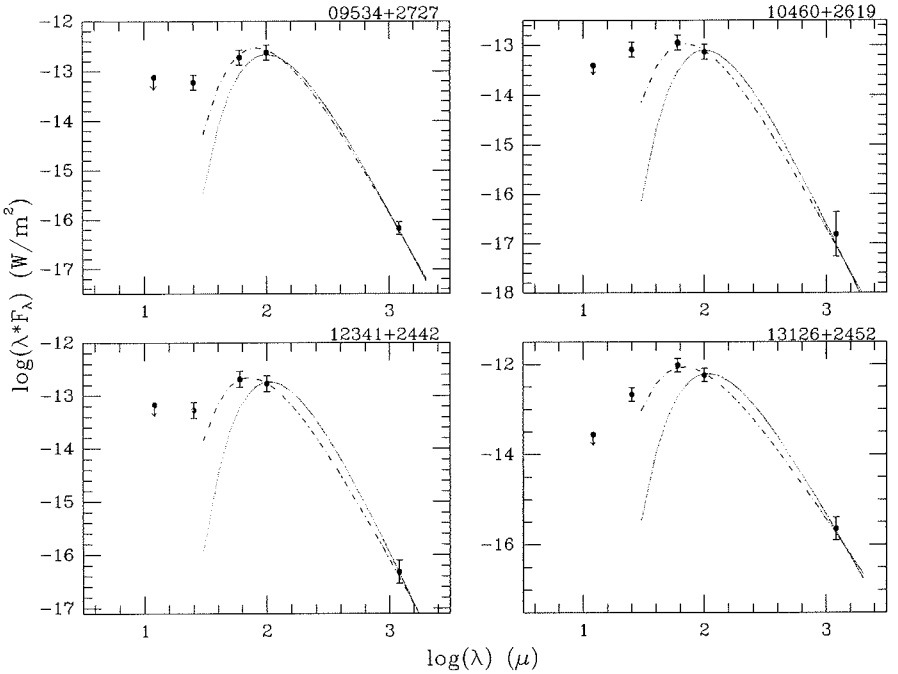

Figure 1: *IR/mm spectra of 4 of the observed galaxies. The 12, 25, 60 and 100 μm data have been taken from the IRAS P.S.C. (see text for details). Two thermal curves $\lambda^{-\alpha} B_\lambda(T_d) \sim 30 \div 40$ K ($\alpha \sim 1 \div 1.5$) (dot-dashed lines) and at $T_d \sim 20$ K ($\alpha \sim 2$) (dotted lines) are shown for comparison.*

where ν_1 and ν_2 are the lower and upper limits on the system spectral response; I_{atm} (ν, w) is the atmospheric emission, assumed to follow a cosecant law: $I = I_o e^{-\tau_o(w)\mathrm{cosec}El}$, $\tau_o(w)$ is the measured zenith optical depth for a given value of the water vapour content w, El is the elevation of the source; ε(ν, El) is the antenna efficiency and Υ(ν) is the optics transmission. The underlying assumption is that the spectra in the millimetric region can be approximated by $F = F_o(\frac{\nu}{\nu_o})^{\alpha}$, where α is the spectral index of the source.

A further correction applied to the millimetric fluxes, due to the different size between the beam width and the optical diametre, has been applied by assuming that the IR disk obeys an exponential law: $I(r) = I_o\exp(-r/r_o)$, $\tau(r) = \tau_o\exp(-r/r_o)$ (Xu and de Zotti, 1989; Bicay and Helou, 1990) and that the IR and mm emissions are spatially correlated (see for instance Andreani et al., 1990).

In Figure 1 is also reported a fit with a modified Planck spectrum $\lambda^{-\alpha} B_\lambda(T_d)$ with α ranging between ~1.0 and 1.5 and $T_d \sim 30 \div 40$ K (dot-dashed line). However, the solution is not unique because very likely the 60 μm point is affected by emission of smaller dust grain at a much larger equilibrium temperature. In fact, by excluding the 60 μm point the curve matching the data has a lower temperature, $T_d \sim 20$ K and $\alpha \sim 2$ (dotted line). Note that, in order to infer a value for the dust temperature, the spectral index must be fixed and this can be done only by adopting a dust model. In this case we used the values of $1 \div 2$ as predicted by the most accepted models (e.g. Draine and Lee, 1984).

Dust and Gas Masses

The thermal emission from dust at these wavelengths is optically thin, therefore one samples the entire line of sight and determines the total dust column density; at mm and submm wavelengths the flux density, F_λ, depends linearly on the dust mass and its temperature (Draine, 1989):

$$F_\lambda \simeq \frac{2kc\sum_i \chi_i(\lambda) < T_i > M_d}{\lambda^4 D^2} \quad (1)$$

where $\chi_i(\lambda)$ are the grain opacities due to component i; $< T_i >$ is the time-average temperature (at these wavelengths it is possible to approximate the temperature distribution of the grains with a single temperature) and M_d is the dust mass. Gas masses are then obtained by adopting the relationship between the dust optical depth τ_ν and the hydrogen column density $N(H_2 + HI)$ given by the models.

We estimated the dust masses of the clouds by using two different models of interstellar dust (Draine and Lee, 1984; Mathis and Whiffen, 1989). These models provide values for the grain opacities at 1 mm using different composition and dimensions of dust grains. Draine and Lee (1984) assume that dust grains consist of a mixture of spherical silicates and graphites with size distribution: $\int(a)da \propto a^{-3.5}\, da$ for *a* varying between 50 Å and 0.1 μm. Mathis and Whiffen (1989) model grains as fluffy aggregates of submicron-size particles composed of various astronomical minerals whose spatial structure is fractional and chemical composition inhomogeneous. Therefore, grains can attain greater dimensions (from 0.03 μm up to ~1 μm).

By using eq. (1) we find for the 7 sources of the sample the values listed in Table 1. For each source both the cold dust component (from 1.2-mm observations), the warm component (from 100 μm IRAS data) and the evaluated values for the gas masses are reported. The first row contains values deduced from the Mathis and Whiffen's model,

TABLE 1: *Estimated dust and gas masses (in $M_\odot$)*

Galaxy	Cold dust (mm)	Warm dust (IR)	M_{gas}	M(HI)
09534+2727	$*(1.9 \pm 0.3)10^6$ $\dagger(4.6 \pm 0.7)10^6$	$*(6.4 \pm 0.3)10^5$ $\dagger(8.6 \pm 1.3)10^5$	$*8.1\ 10^8$ $\dagger 4\ 10^9$	$3.7\ 10^8$
10460+2619	$*(2.3 \pm 1.0)10^7$ $\dagger(5.5 \pm 2.3)10^7$	$*(4.5 \pm 0.7)10^6$ $\dagger(6.0 \pm 0.9)10^6$	$*10^{10}$ $\dagger 1.3\ 10^{10}$	$5.7\ 10^9$
12341+2442	$*(4.4 \pm 1.0)10^7$ $\dagger(1.1 \pm 0.3)10^8$	$*(7.3 \pm 1.1)10^6$ $\dagger(9.8 \pm 1.5)10^6$	$*2\ 10^{10}$ $\dagger 3.9\ 10^{10}$	$5.4\ 10^9$
13126+2452	$*(8.3 \pm 2.1)10^7$ $\dagger(2.0 \pm 0.5)10^8$	$*(5.4 \pm 0.8)10^6$ $\dagger(7.3 \pm 1.1)10^6$	$*3.4\ 10^{10}$ $\dagger 10^{11}$	–
13387+2331	$*(8.2 \pm 3.1)10^7$ $\dagger(2.0 \pm 0.8)10^8$	$*(1.4 \pm 0.2)10^7$ $\dagger(1.9 \pm 0.3)10^7$	$*4.2\ 10^{10}$ $\dagger 10^{11}$	–
15373+2506	$*(3.7 \pm 2.1)10^7$ $\dagger(8.9 \pm 5.1)10^7$	$*(5.4 \pm 0.8)10^6$ $\dagger(7.2 \pm 1.1)10^6$	$*1.8\ 10^{10}$ $\dagger 4\ 10^{10}$	–
15566+2657	$*< 1.8\ 10^7$ $\dagger < 4.3\ 10^7$	$*(1.3 \pm 0.2)10^6$ $\dagger(1.8 \pm 0.3)10^6$	$*< 7.8\ 10^9$ $\dagger < 4.3\ 10^{10}$	$4.3\ 10^8$

* Values deduced from Mathis and Whiffen's model.
† Values deduced from Draine and Lee's model.
M(HI) are taken from the literature (see text).

and the second row those inferred from Draine and Lee's computations. When available, the M(HI) masses calculated by using HI 21 cm data are listed in the fifth column (Bicay and Giovanelli, 1987; Mirabel and Sanders, 1988; Young et al. 1989).

Discussion and Conclusion

The main advantages on the determinations of the dust mass at these wavelengths lie on a better evaluation of $< T_i >$ since at higher frequency the uncertainties in the temperature distribution function may introduce order-of-magnitude errors in $< B_\lambda(T) >$.

Note that the warm dust masses listed in Table 1 can be underestimated also because the IRAS 100 μm measurements do not fully sample the total dust in the galaxy disk.

However, the uncertainties in the grain opacities are larger at long wavelengths even if they do not depend on the details of the size distribution. Gas and dust masses are estimated, then, within a factor of 5 (see Table 1).

The comparison with M(HI) suggests that very likely there is a substantial contribution to the total gas mass due to H_2. But, to draw any firm conclusion on this point we need CO line measurements of these galaxies, which up to now have not been carried out.

Young et al. (1989) found that for a sample of IRAS spirals $M(H_2)$ ranges between 10^8 and $5 \cdot 10^{10}$ $M_\odot$ and the ratio $M(H_2)/M(HI)$ is of the order of 1. If this is the case also for the observed sources of our sample, the gas mass values inferred from our measurements would agree with those determined from CO and HI data.

It should be stressed that the approach used here is not claimed to be, up to now, of greater accuracy than other determinations of gas masses (e.g. using the integrated intensity of the ^{12}CO line) but it is important either because it implies a completely independent method based on a different set of assumptions. However, these observations can substantially improve our knowledge on dust opacities at long wavelengths and constrain models of dust grains. This would turn into a better determination of dust and gas masses.

Therefore, we find this approach more promising with respect to that based on CO line intensities since the uncertainties related to this latter are largely connected to the physical conditions of the medium and then more difficult to evaluate.

Further observations will be carried out at SEST in September and they will be helpful in gaining statistical insights into these problems.

Acknowledgements

We would like to warmly thank Dr. H. Steppe for his kind introduction at the IRAM 30-m antenna and help during the observations, Dr. E. Kreysa for helpful suggestions and all IRAM staff for technical support. P.A. thanks ESO for the hospitality during the CNR fellowship supporting this work.

References

P. Andreani et al., 1990, *Astroph. J.* **348,** 467.
M.D. Bicay and R. Giovanelli, 1987, *Astron. J.,* **93,** 1326.
M.D. Bicay and G. Helou, 1990, to appear in *Astroph. J.,* October.
R. Chini et al., 1986, *Astron. Astroph.,* **166,** L8.
B.T. Draine, 1989, in *The interstellar medium in galaxies,* ed. H.A. Thronson and J.M. Shull, Dordrecht: Kluwer, in press.
B.T. Draine and H.M. Lee, 1984, *Astroph. J.,* **285,** 89.
S.A. Eales et al., 1989, *Astroph. J.,* **339,** 859.
A. Franceschini et al., 1989, *Astroph. J.,* **334,** 35.
W.K. Gear et al., 1985, *Astroph. J.,* **291,** 511.
C.J. Lonsdale et al., 1989, *Cataloged Galaxies and Quasars observed in the IRAS survey,* version 2, Jet Propulsion Laboratory.
J.S. Mathis and G. Whiffen, 1989, *Astroph. J.,* **341,** 808.
I.F. Mirabel and D.B. Sanders, 1988, *Astroph. J.,* **335,** 104.
G.S. Orton et al., 1986, *Icarus,* **67,** 289.
B.J. Smith et al., 1987, *Astroph. J.,* **318,** 161.
A. Stark et al., 1988, *Astroph. J.,* **337,** 650.
J.S. Young et al., 1989, *Astroph. J. Suppl.,* **70,** 699.
C. Xu and G. De Zotti, 1989, *Astron. Astroph.,* **225,** 12.

Variability as a Way to Find Quasars: a Complete Sample

M. HAWKINS, Royal Observatory Edinburgh, United Kingdom
P. VÉRON, Observatoire de Haute-Provence, France

Introduction

To study the cosmological evolution of quasars, it is first necessary to establish a complete sample. This has proved to be particularly difficult, for several reasons. Early work was based on radio surveys, and although this resulted in well defined samples with no obvious bias in redshift, it was inevitably limited to a small subset of quasars (1 or 2%) which themselves showed a wide variety of radio properties. Most recent results are based on samples obtained by two main methods: the UV excess method (see Véron, 1983, for a review), later generalized to the multicolour method (Koo et al., 1986), and the slitless spectroscopy method (see Véron, 1983, for a review). Although both techniques can produce samples apparently containing a sizeable fraction of the quasar population, they each suffer the drawback that their detection efficiency is strongly dependent upon redshift. To some extent they may be seen as complementary procedures as the UVX method is most efficient in the low redshift regime, while slitless spectroscopy is more sensitive to high redshift objects. However, what is clearly needed is a selection technique which is essentially independent of redshift, and is capable of detecting a substantial fraction of all quasars brighter than a given flux limit.

Most, if not all, quasars are optically variable. Indeed, previous studies have shown that up to 70% of all quasars have an amplitude of variability larger than 0.43 mag. (Trevese et al., 1989). Van den Bergh et al. (1973) first suggested using this property as a method for finding quasars, and Sanitt (1975) discussed the various types of variable star (RR Lyrae and low-luminosity M-type flare stars) which might contaminate a sample compiled by this method. There are number of advantages in using variability as a search criterion for quasars. There are essentially no instrumental redshift biases, and apart from some constraints set by the passband of the search, there are no colour- or magnitude-dependent biases. Set against this, there is the practical limitation that the timescale of variation for most quasars is several years and so a search must be undertaken over a decade or more to detect a reasonably high fraction of the quasar population.